Journal of Hazardous Materials B109 (2004) 183–189

Journal of Hazardous Materials

www.elsevier.com/locate/jhazmat

Removal of sulfur dioxide from a continuously operated binary fluidized bed reactor using inert solids and hydrated lime

R. Pisani, Jr. [a,*], D. de Moraes Jr. [b,1]

[a] *Post-Graduate Program in Environmental Technology, University of Ribeirão Preto, Rua José Bonifácio 799, CEP: 13560-610, São Carlos, SP, Brazil*
[b] *University of Santa Cecília, Rua Oswaldo Cruz, 266, CEP: 11045-907, Boqueirão, Santos, SP, Brazil*

Received 6 November 2003; received in revised form 18 March 2004; accepted 18 March 2004

Available online 5 May 2004

Abstract

Sulfur dioxide pollutant was treated in the laboratory with hydrated lime particles having a mean diameter of 9.1 μm in a continuously operating binary fluidized bed reactor also containing inert sand particles with sizes varying from 500 to 590 μm. The influence of temperature (500, 600, 700 and 800 °C) on the reaction medium, of the superficial velocity of the gas (0.8, 1.0 and 1.2 m/s), and of the Ca/S molar ratio (1, 2 and 3) on the SO_2 removal efficiency were investigated for an inflow gas concentration of 1000 ppm and an initially static bed height of 10.0 cm. The pollutant removal efficiency proved to depend on the temperature and the velocity of the gaseous flow and was strongly influenced by the Ca/S molar ratio. The maximum efficiency of 97.7% was achieved at a temperature of 700 °C, a Ca/S ratio of 3 and a velocity of 0.8 m/s. The lime particles' mean residence time was determined by an indirect method, which consisted of integrating the gas concentration curves normalized with respect to time. Based on a calculation of the critical transition velocities, it was concluded that the reactor operated in a bubbling regime under each condition investigated here.

Keywords: Powder-particle fluidized bed; Sulfur dioxide; Bubbling fluidization; Gas–solid reaction; Hydrated lime

1. Introduction

Sulfur dioxide is a toxic gas with a strong odor, an irritant that can be fatal in cases of acute exposure [1]. This gas causes systemic disorders such as nasopharyngitis, chronic bronchitis, fatigue and alterations of the sense of smell. Being water soluble, its local effects on the human body are manifested mainly as respiratory disorders [2].

Because it produces high contents of sulfur, the combustion of mineral coal and petroleum by-products in thermoelectric power plants and industrial furnaces and boilers contributes toward one of the most problematic forms of pollution—acid rain. Sulfur dioxide is also generated by processing plants, e.g., pulp and paper plants, tanneries, copper ore works and sugar mills, as well as by units treating hydrogen sulfide and mercaptans by incineration.

The noncatalytic dry treatment of this pollutant consists basically of promoting the reaction of the gas with a solid alkali, usually CaO, at temperatures of approximately 800 °C. At the temperatures at which this process is efficient (700–850 °C), this reaction produces calcium sulfate, especially in the presence of excessive amounts of oxygen [3–8]. The global reaction can be expressed as:

$$CaO_{(s)} + SO_{2(g)} + \tfrac{1}{2}O_{2(g)} \rightarrow CaSO_{4(s)}$$

CaO is obtained from the calcination of abundant and low cost raw materials such as calcitic limestone, dolomitic limestone and hydrated lime. The calcination of these materials implies the formation of a porous structure resulting from the release of the carbonates' CO_2 and the hydroxides' H_2O.

In the chemical reaction between the porous particles and the gaseous reagents (SO_2 and O_2), the solid product is formed preferentially inside the pores of the particles close to the surface, leaving the central region unaltered. This class of chemical reaction has been described in the literature by "Shrinking Core" type models in innumerable studies developed in the 1970s and improved upon to this day [3,9–16].

* Corresponding author. Tel.: +55-16-271-0658; fax: +55-16-603-7002.
E-mail addresses: pisanijr@terra.com.br (R. Pisani Jr.), deovaldo@unisanta.br (D. de Moraes Jr.).
[1] Tel.: +55-13-3202-7100x144; fax: +55-13-3202-7132.

0304-3894/$ – see front matter © 2004 Elsevier B.V. All rights reserved.
doi:10.1016/j.jhazmat.2004.03.005

Nomenclature

C	concentration of SO_2 at the exit at each instant (ppm)
C_f	arithmetic average of the SO_2 concentration at the exit between 55 and 60 min of operation in the permanent regime (ppm)
C_0	initial concentration of SO_2 (ppm)
d_p	particle size by equation 3 (m)
d_{sf}	diameter of the fine particles (m)
d_{sg}	diameter of the coarse particles (m)
D	diameter of the column of the bed (m)
g	acceleration of gravity (m/s^2)
m_{lime}	mass outflow of hydrated lime at the entrance (g/min)
p	rotation period of the screw (s)
r	correlation coefficient (nondimensional)
R	internal radius of the column (m)
t_f	time of the experiment (min)
T	temperature of the reactor (°C)
u_c	critical transition velocity in the bubbling regime for turbulence (m/s)
V	superficial velocity of the gas (m/s)
W	constant
x_c	mass fraction of large particles in the bed
X	SO_2 removal fraction (%)
μ	absolute viscosity of the gas (kg/(m s))
$\mu_{20\,°C}$	absolute viscosity of the gas at 20 °C (kg/(m s))
ρ_g	specific mass of the fluidization gas (kg/m^3)
$\rho_{g20\,°C}$	specific mass of the fluidization gas at 20 °C (kg/m^3)
ρ_{sf}	specific mass of the fine particles (kg/m^3)
ρ_{sg}	specific mass of the thick particles (kg/m^3)
θ	mean residence time of the solid reagent inside the bed (min)

The physical properties of the calcined particle, such as specific surface area, porosity and pore size distribution, are strongly influenced by the calcining conditions, such as time and temperature, and by the type of raw material employed. Solids whose structure is less dense prior to calcination normally have a greater sulfatizing capacity [9,10,17].

Comparative studies carried out on different reactors have revealed that hydrated lime supplies higher sulfate conversions than do calcitic and dolomitic lime [7,18,19]. Al-Shawanekeh et al. [19], for instance, obtained maximum conversions of 71 and 61% for calcium oxide generated, respectively, from hydrated lime and from limestone, at a temperature of 850 °C and 3100 ppm of SO_2.

Fine particles have a larger surface area and are less resistant to the diffusion of gases through the porous structure of the solid; hence, their use is recommended as a source of CaO for the treatment of SO_2. However, limestone and hydrated lime particles with diameters of less than 50 μm are classified as belonging to Geldart's C group [20] and therefore fluidize with a strong tendency for agglomeration and can easily be dragged off a fluidized bed owing to the low terminal velocity.

Kato et al. [21] proposed the use of SO_2 treatment on a powder-particle fluidized bed. In this system, the fine solid reagent, normally having a diameter of less than 50 μm, is fed continuously to a fluidized bed of thick inert particles so that only the fine ones are continually elutriated. This allows the operation to take place at higher superficial velocities, since the conditions for fluidization are defined almost exclusively by the properties of the thick particles. These researchers treated SO_2 on a bench scale with the addition of calcitic limestone, using thick sand particles with diameters of 495–991 μm, and fine limestone particles with 2, 5 and 9.9 μm diameters, and studying the influence of temperature (650–950 °C), of the molar ratio of Ca/S (1, 2 and 3), the superficial velocity of the fluidization gas (1.0, 1.5, 2.0 and 2.5 m/s), the height of the initially static bed (10.0, 20.0 and 30.0 cm), and the inflow concentration of SO_2 (500, 700 and 1000 ppm).

These authors found that the SO_2 removal efficiency was considerably dependent on the variables investigated, achieving 100% removal at a temperature of 800 °C, with a limestone particle diameter of 5 μm, a Ca/S molar of 2.5, a static bed height of 10.0 cm, superficial velocity of 1.0 m/s, and inflow gas concentration of 1000 ppm. However, they did not classify the fluidization regime for the conditions they studied, nor did they propose a model to describe the process.

Operating the same system as Kato et al. [21] but using 29 μm dolomitic limestone particles and a (Ca + Mg)/S molar ratio of 2, Tashimo et al. [22] achieved a removal efficiency of approximately 50% at a temperature of 800 °C, a velocity of 1.0 m/s, static bed height of 10.0 cm and inflow gas concentration of 1000 ppm, as opposed to the 65% achieved by Kato et al. [21] with 5 μm calcitic limestone particles and a Ca/S molar ratio of 2 under the same conditions.

Tashimo et al. [22] found that the effect of the concentration of CO_2 in a range of 0–20% volume, which is normal for combustion gases, hardly affected the SO_2 removal efficiency, particularly in the presence of large amounts of solid reagent (Ca/S ratios of 2 and 3 and (Ca + Mg)/S of 2). They concluded that the particle size of the solid reagent exerted a significant influence. The gas removal efficiency, for instance, dropped from 85%, achieved with the 2.9 μm dolomitic limestone, to 40%, using the same limestone with a diameter of 53 μm, under the same operating conditions.

As can be seen from the above, the conditions whereby contact occurred between the gaseous and solid phases dictated directly in the performance of the process, indicating the need to determine the fluidization regime for the system's operating conditions.

Kunii and Levenspiel [23] gave a detailed description of fluidization regimes, finding, as did other researchers, that

the transition from one regime to another occurred according to the superficial velocity of the gaseous flow and the properties of the solid in suspension. They also found that a mix of solids in a bed can be defined by determining the fraction of fine and coarse particles it is composed of and their physical properties. The mass of fine particles retained in the bed can be identified by the mass feed flow multiplied by the mean residence time.

Kato et al. [24] investigated the behavior of the average residence time of fine solids in a binary bed composed of alumina particles, the large ones with diameters of 399, 505 and 605 μm and the small ones 6.5–16.2 μm. However, the velocities they used (0.09–0.27 m/s) were close to those of the bed's minimum fluidization.

Recently, Pisani and Moraes [25] treated SO_2 using dolomitic limestone (24 μm) in a binary fluidized bed reactor composed of 500–590 μm diameter sand particles. They obtained a maximum gas removal fraction of 76% under the following conditions: superficial velocity of 0.8 m/s, temperature of 800 °C and a Ca/S ratio of 3 for a SO_2 concentration of 1000 ppm and a static bed height of 10 cm. These researchers estimated average reagent particle residence times of 4–14 min, finding their values were little influenced by the superficial velocity of the gas under the conditions employed and concluding that the reactor operated in a bubbling regime under all the operating conditions studied.

The main objectives of this study were to experimentally determine the SO_2 removal fraction as a function of the operating temperature, the superficial fluidization velocity, the Ca/S ratio achieved with continuous hydrated lime feeding under a steady state, and the definition of the existing fluidization regime.

2. Materials and methods

2.1. Fluidization regime

Empirical correlations are useful to calculate the critical transition velocity of the bubble regime for the turbulence (u_c) because it takes into account the influence of the temperature on the physical properties of the gas and the composition of the particle mixture in the bed.

Cai et al. [26] proposed an equation to calculate u_c based on innumerable experiments performed in the pressure interval of 0.1–0.8 MPa, from ambient temperature to 500 °C, for eight types of particles with diameters ranging from 53 to 1057 μm and a specific mass of 706–2580 kg/m^3. Bai et al. [27] adapted this equation for use in binary beds, proving its validity through the pressure drop oscillation method.

$$\frac{u_c}{\sqrt{g d_p}} = \left(\frac{\mu_{20\,^\circ C}}{\mu}\right)^{0.2} \times \left[W\left(\frac{\rho_{g\,20\,^\circ C}}{\rho_g}\right)\left(\frac{\rho_s - \rho_g}{\rho_g}\right)\left(\frac{D}{d_p}\right)\right]^{0.27} \quad (1)$$

$$W = \left(\frac{0.211}{D^{0.27}} + \frac{0.00242}{D^{1.27}}\right)^{1/0.27} \quad (2)$$

$$d_p = \frac{1}{(1 - x_c)/d_{sf} + (x_c/d_{sg})} \quad (3)$$

$$\rho_s = \frac{1}{(1 - x_c)/\rho_{sf} + (x_c/\rho_{sg})} \quad (4)$$

This set of equations requires knowledge of the fraction of fine solids retained in the bed to calculate x_c and hence, u_c. However, this requirement can be bypassed by knowing the mean residence time (θ) of the fine solids inside the binary bed. The mass fraction of large particles (1029 g) in the mixture that makes up the bed (x_c), shown in Eqs. (3) and (4), can be calculated by:

$$x_c = \frac{1029\,g}{1029\,g + \theta m_{cal}} \quad (5)$$

We propose that the mean residence time of the solid reagent (θ) in the reactor be calculated by integrating the SO_2 concentration curves normalized as a function of time in the transient regime analogously to a step signal, since there are continuous inflows of gas and fine solid reagent and continuous outflows of gas and fine solid reagent continually dragged by the gas. Moreover, the mass of sand contained in the column (1029 g) is sufficiently large to allow one to disregard an increment of the total particulate mass in the bed owing to the increase in lime mass in the bed during this period.

$$\theta = \int_0^{t_f} \left(\frac{C - C_f}{C_0 - C_f}\right) dt \quad (6)$$

The main simplifications of this approach are: negligible gaseous phase residence times (lower than 1.5 s) in relation to the stay time of the solid reagent, linear behavior of the consumption of solid and gaseous reagents, constant mass of solids in suspension (practically the mass of sand). Therefore, the reduction in SO_2 concentration at the exit can be instantaneously attributed to the increase in the concentration of solid reagent in the bed.

The mass outflow of hydrated lime was obtained from the equation of the ideal gas state, the stoichiometric balance and its chemical composition.

The SO_2 removal fraction (X) was defined by:

$$X(\%) = \frac{(C_0 - C_f)}{C_0} \times 100 \quad (7)$$

2.2. Equipment and accessories

The column consisted of a 316 stainless steel tube with an internal diameter of 85 mm and a total height of 1.0 m. The inert bed was composed of 500–590 μm diameter sand particles and an initially static height of 10.0 cm measured from the point where the solid reagent feeder was coupled to the column, with a total height of 12.0 cm. Fig. 1 shows a diagram of the equipment used in this study.

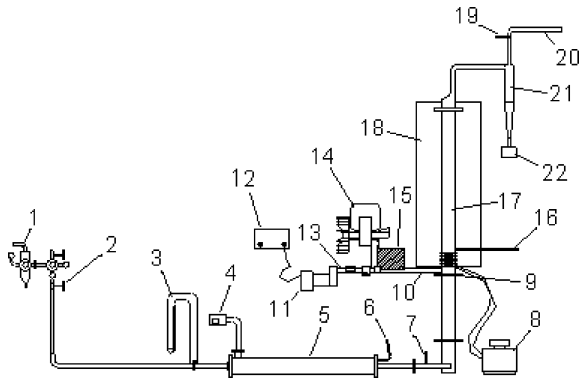

Fig. 1. Diagram of the equipment: (1) pressure reduction valve; (2) needle valve; (3) manometer and orifice meter; (4) PID temperature controller; (5) electric heater; (6) temperature sensor; (7) SO_2 entrance; (8) current amperage variation device; (9) gas distributor plate; (10) screw feeder; (11) electric motor; (12) rotation variation device; (13) rotation counter; (14) vibrator; (15) solid reagent receptacle; (16) temperature sensors; (17) column; (18) thermal insulator; (19) gas sampling port; (20) exhaust outlet; (21) cyclone; (22) receptacle for holding collected particulate material.

The equation for calibration of the solid reagent feeder for the mass outflow of hydrated lime was:

$$m_{\text{lime}} = 6.831 \times p^{-0.9381} \quad (8)$$

where $2.0\,\text{s} \leq p \leq 32.3\,\text{s}$.

The fluidization gas distributor located under the solids feeder consisted of a perforated plate with 1% of the free area of the column's transversal section.

The concentration of SO_2 at the entrance was kept constant in each experiment, i.e., close to 1000 ppm, using a rotameter and a needle valve.

The SO_2 concentration was measured with a Horiba, model PG 250 analyzer with a precision of 1% from the bottom of the scale and the smallest division being 1 ppm, as well as a data acquisition system that recorded the concentration values at 10 s intervals. The analytical method employed in the analyzer was infrared radiation absorption.

The temperature was measured at nine points located in three radial (0, $R/2$ and $3R/4$) and five axial (13.5, 27.0, 50.0, 73.5 and 96.0 cm) positions.

The hydrated lime was granulometrically analyzed using a Malvern Mastersizer device, which supplied the median diameter of 9.1 μm. A Micrometrics, model Accupyc 1330 helium pycnometer was used to measure the specific mass of the lime and sand, which were, respectively, 2610 and 2638 kg/m^3.

The hydrated lime was chemically characterized by differential thermal analysis and atomic emission spectrometry. Table 1 shows the average composition obtained.

2.3. Experimental procedure

The experimental procedure used is described in detail by Pisani and Moraes [25].

Table 1
Average chemical composition of the hydrated lime used

Compound	Mass (%)
$Ca(OH)_2$	46.0
$CaCO_3$	31.4
CaO	3.8
MgO	7.4
$Mg(OH)_2$	6.6
$MgCO_3$	1.3
Impurities	3.5
Total	100.0

3. Results and discussion

The 36 experiments carried out in this study revealed the same behavior for the SO_2 concentration at the exit as a function of time, as shown in Fig. 2.

The concentration of SO_2 showed a conspicuous drop under every experimental condition, indicating the consumption of the gaseous reagent under these conditions. The temperature of the dehydroxilation reaction of the hydrated lime, performed in a thermobalance, was 450 °C [28]; therefore, CaO was available for the reaction with SO_2 under each of the operating conditions tested.

It was also generally found that the system required approximately 45 min to enter the steady state; hence, the 60 min time used in this methodology was appropriate. Interrupting the hydrated lime feed after 60 min of operation enabled us to verify the tendency for the outgoing concentration to return to the initial concentration, and the 30 min interval was, in some instances, insufficient, particularly when a greater amount of gas was removed. However, in the first moments after the interruption, the marked increase in SO_2 concentration indicated the loosening of a large part of the lime particles from the bed during that period.

Fig. 3 depicts the typical behavior obtained with the residual SO_2 concentration curves normalized as a function of time, utilized to calculate the mean residence time of the solid reagent particles in the reactor.

These curves were integrated (Eq. 6) using the Microcal Origin 4.0 software application and the results of the mean residence time of the solid reagent, the mass fraction of sand

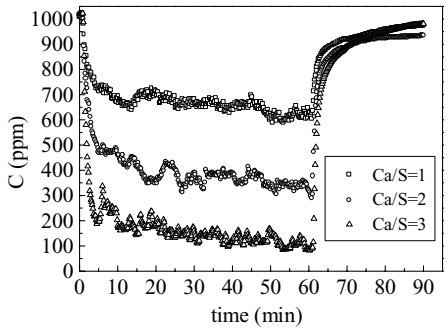

Fig. 2. SO_2 concentration curves at the exit as a function of time for a temperature of 600 °C and 0.8 m/s superficial velocity of the gaseous flow.

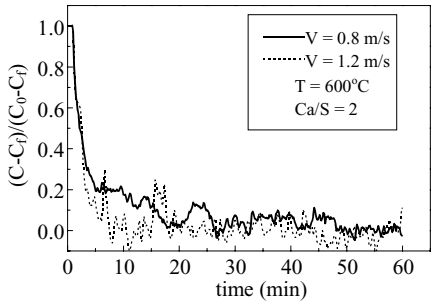

Fig. 3. SO_2 concentration curves normalized as a function of time at a temperature of 600 °C and Ca/S molar ratio of 2.

(Eq. 5) and the critical transition velocity (Eqs. (1)–(4)) are given in Tables 2, 3 and 4.

Fig. 3 shows a slight tendency for reduction of the residual concentration of SO_2 normalized with the increase in the superficial velocity of the gas, a phenomenon that was reflected in the results of θ (Tables 2, 3 and 4). It was found that higher temperatures contributed little toward increasing the lime's residence time in the bed at velocities of 0.8 and 1.0 m/s (Tables 2 and 3), an effect that was relevant only at a velocity of 1.2 m/s (Table 4). This behavior, coupled with the fact that the residence times of the lime were approximately 100–650 times longer than those of the gaseous phase, indicated that the viscous and inertial effects of gas drainage are secondary under these conditions, and that the interaction among large particles (sand) and small ones (lime) should be the predominating mechanism.

Table 2
Results of u_c, x_c and θ as a function of the operating conditions at a velocity of 0.8 m/s

	T (°C)	m_{lime} (g/min)	θ (min)	x_c	u_c (m/s)
Ca/S = 1, 0.8 m/s	500	0.39	4.6	0.998	1.56
	600	0.35	8.2	0.997	1.62
	700	0.31	12.4	0.996	1.68
	800	0.28	13.6	0.996	1.75
Ca/S = 2, 0.8 m/s	500	0.79	8.4	0.994	1.48
	600	0.70	6.2	0.996	1.59
	700	0.63	8.2	0.995	1.65
	800	0.57	7.6	0.996	1.74
Ca/S = 3, 0.8 m/s	500	1.18	6.7	0.992	1.47
	600	1.05	4.8	0.995	1.58
	700	0.94	5.1	0.995	1.66
	800	0.85	7.1	0.994	1.71

Table 3
Results of u_c, x_c and θ as a function of the operating conditions at a velocity of 1.0 m/s

	T (°C)	m_{lime} (g/min)	θ (min)	x_c	u_c (m/s)
Ca/S = 1, 1.0 m/s	500	0.49	3.7	0.998	1.56
	600	0.44	5.2	0.998	1.63
	700	0.39	7.2	0.997	1.70
	800	0.35	8.9	0.997	1.76
Ca/S = 2, 1.0 m/s	500	0.98	8.4	0.992	1.46
	600	0.87	6.5	0.995	1.57
	700	0.78	6.8	0.995	1.65
	800	0.71	7.0	0.995	1.73
Ca/S = 3, 1.0 m/s	500	1.48	5.8	0.992	1.46
	600	1.31	3.0	0.996	1.60
	700	1.17	4.4	0.995	1.65
	800	1.06	5.8	0.994	1.71

Table 4
Results of u_c, x_c and θ as a function of the operating conditions at a velocity of 1.2 m/s

	T (°C)	m_{lime} (g/min)	θ (min)	x_c	u_c (m/s)
Ca/S = 1, 1.2 m/s	500	0.59	8.0	0.995	1.51
	600	0.52	4.9	0.998	1.63
	700	0.47	8.1	0.996	1.68
	800	0.43	11.3	0.995	1.73
Ca/S = 2, 1.2 m/s	500	1.18	1.5	0.998	1.56
	600	1.05	3.1	0.997	1.61
	700	0.94	4.6	0.996	1.67
	800	0.85	6.3	0.995	1.72
Ca/S = 3, 1.2 m/s	500	1.77	2.7	0.995	1.51
	600	1.57	3.7	0.994	1.57
	700	1.41	6.6	0.991	1.59
	800	1.28	6.9	0.992	1.66

No studies were found in the literature using similar experimental conditions that would allow for a comparison of the results of θ obtained here.

Knowing the values of θ and x_c made it possible to calculate the critical transition velocity, whose values ranged from 1.46 to 1.76 m/s, allowing the bed's fluidization to be classified as bubbling under each experimental condition employed, since the superficial velocities used here were 0.8–1.2 m/s.

Figs. 4–6 illustrate the results of the pollutant removal fraction as a function of operational conditions.

Probably owing to its pores' larger specific surface area and diameter, the hydrated lime showed larger SO_2 removal fractions than did the dolomitic limestone used by Pisani and Moraes [25] under all the conditions studied, a behavior that was congruent with the results of Al-Shawanekeh et al. [7,19], obtained in thermobalances.

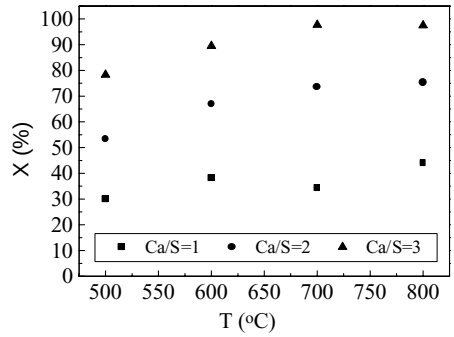

Fig. 4. SO_2 removal fraction as a function of temperature and Ca/S ratio for a velocity of 0.8 m/s.

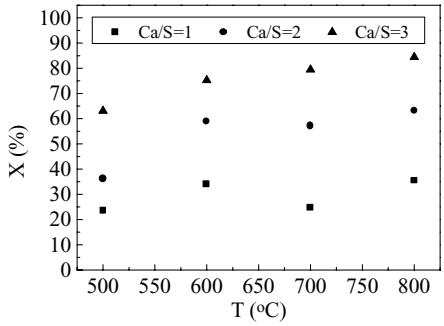

Fig. 5. SO_2 removal fraction as a function of temperature and Ca/S ratio for a velocity of 1.0 m/s.

The gas removal fraction increased with a decreasing slope as a function of temperature. The rise in temperature accelerated the sulfation rate, since the hydrated lime dehydroxilation temperature was 450 °C [28]. However, at high conversions of CaO to $CaSO_4$, the layers of the product on the external part of the reagent particles and inside the pores can become a physical barrier to mass transfer, which, in this case, takes place mainly through product layer diffusion [18,29,30].

The increase in the superficial velocity of the gaseous flow led to a reduction of the SO_2 removal fraction. At 700 °C and a Ca/S ratio of 3, for instance, the values of X dropped from 97.7% at 0.8 m/s (Fig. 4) to 79.4% at 1.0 m/s (Fig. 5), and 73.4% at 1.2 m/s (Fig. 6). This behavior may be explained by the reduction of the mean residence time in the gaseous phase or of the mass fraction of solid reagents retained in the bed. At a velocity of 0.8 m/s, the average residence time of gas inside the reactor (column) was 1.25 s and at a velocity of 1.2 m/s, it was 0.83 s, which implied shorter contact and reaction times between phases. On the other hand, an increase in the superficial velocity of the gas would reduce the amount of solid reagent retained in the fluidized sand bed owing to increased entrainment of fine particles. However, this was not found in our calculation of x_c, since the mass fractions of sand in the bed (x_c), for example, were 0.995 at 0.8 m/s (Table 2), 0.995 at 1.0 m/s (Table 3) and 0.991 at 1.2 m/s (Table 4) under the aforementioned conditions. Hence, the decreasing behavior of the SO_2 removal fraction as a function of superficial velocity was justified by the reduction in the average residence time of the gaseous phase inside the reactor.

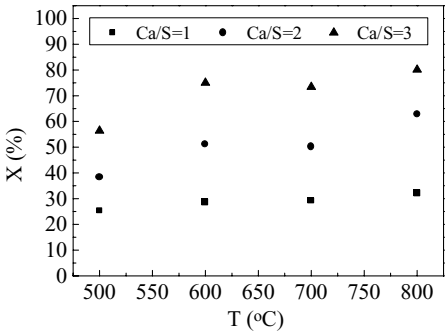

Fig. 6. SO_2 removal fraction as a function of temperature and Ca/S ratio for a velocity of 1.2 m/s.

Table 5
Results of the repeat tests of the gas removal fraction

Test	$T = 500$ °C, Ca/S = 1, V = 0.8 m/s	$T = 700$ °C, Ca/S = 2, V = 1.0 m/s	$T = 800$ °C, Ca/S = 3, V = 1.2 m/s
1	30.0	57.1	80.1
2	27.2	57.7	82.1

Table 5 lists the results of the repeat tests in relation to the gas removal fraction, showing that the tests were reproduced sufficient times to compromise neither the quality of the results presented here nor the validity of this discussion.

4. Conclusions

This study involved the effective treatment of SO_2 pollutant, in which the pollutant removal fraction proved dependent on the temperature of the reaction medium and on the superficial velocity of the gas flow, and was strongly influenced by the molar ratio of Ca/S. The maximum fraction of approximately 98% was obtained at 700 °C, a Ca/S molar ratio of three and a superficial velocity of 0.8 m/s.

The method proposed here allowed for the mean residence time of the reagent particles in the bed to be estimated, and the values obtained in the interval of 1.5–13.6 min were little influenced by the operating conditions at gas flow velocities of 0.8 and 1.0 m/s, as well as considerably higher than the average residence time of 0.8–1.2 s of the gaseous phase inside the column. At a velocity of 1.2 m/s, the mean residence time of the fine particles tended to increase with temperature, a behavior that was attributed to the viscous and inertial effects of the gas in the predominant effect of interaction by contact between the small and large particles in the bed.

From the calculation of the critical transition velocities, it was concluded that the reactor operated in a bubbling regime under all the conditions studied and that the increase in average residence time of the gas flow in the reactor explained the increasing SO_2 removal efficiency as a function of the reduction in the superficial velocity of the gas.

References

[1] M. Galea, Fatal sulfur dioxide inhalation, Can. Med. Assoc. J. 91 (1964) 345–347.
[2] M.M. Key, Occupational Diseases: a Guide to their Recognition, US Department of Health, Education and Welfare, Washington, 1977.
[3] R.H. Borgwardt, Kinetics of the reaction of SO_2 with calcined limestome, Environ. Sci. Technol. 4 (1970) 59–63.
[4] D.W. Marsh, D.L. Ulrichson, Rate and diffusional study of the reaction of calcium oxide with sulfur dioxide, Chem. Eng. Sci. 40 (1985) 423–433.

[5] A. Lyngfelt, B. Leckner, SO_2 capture in fluidized-bed boilers: re-emission of SO_2 due to reduction of $CaSO_4$, Chem. Eng. Sci. 44 (1989) 207–213.
[6] A. Lyngfelt, V. Langer, B.M. Steenari, K. Puromäki, Calcium sulphide formation in fluidized beds, Can. J. Chem. Eng. 73 (1995) 228–233.
[7] A. Al-Shawanekeh, H. Matsuda, M. Hasatani, Utilization of high improved fly for SO_2 capture, J. Chem. Eng. Jpn. 28 (1995) 53–58.
[8] G. Marbán, M.G. Calzada, B. Fuertes, Kinetics of oxidation of CaS particles in the regime of low SO_2 release, Chem. Eng. Sci. 54 (1999) 77–90.
[9] R.H. Borgwardt, R.D. Harvey, Properties of carbonate rocks related to SO_2 reactivity, Environ. Sci. Technol. 6 (1972) 350–360.
[10] M. Hartman, J. Pata, R.H. Coughlin, Influence of porosity of calcium carbonates on their reactivity with sulfur dioxide, Ind. Eng. Chem. Process Des. Dev. 17 (1978) 411–419.
[11] M.R. Stouffer, H.N. Yoon, A Investigation of CaO sulfation mechanisms in boiler sorbent injection, AlChE J. 35 (1989) 1253–1262.
[12] K.M. Allal, M. Abbessi, A. Mansour, Determination of kinetical data for the reaction of SO_2 with CaO using a thermobalance, Trans. IchemE. 70 (1992) 140–144.
[13] A.B.M. Heesink, W. Prins, W.P.M. Van Swaaij, A grain size distribution model for non-catalytic gas-solid reactions, Chem. Eng. J. 53 (1993) 25–37.
[14] A.E. Meriçboyu, S. Küçükbayrak, Modeling of the sulphation reactions of natural sorbents, Thermochim. Acta 319 (1998) 163–170.
[15] Y. Suyadal, H. Oguz, Dry desulfurization of simulated flue gas in a fluidized bed reactor for a broad range of SO_2 concentration and temperature: a comparition of models, Ind. Chem. Res. 38 (1999) 2932–2939.
[16] S.K. Mahuli, R. Agnihotri, R. Jadhav, S. Chauk, L.S. Fan, Combined calcination, sintering and sulfation model for the $CaCO_3$-SO_2 reaction, AlChE J. 45 (1999) 367–382.
[17] A.M. Hayashi, Estudo do Efeito dos Parâmetros Físicos e Químicos de Adsorvente Sólido no Processo de Adsorção de SO_2 em Calcário, Universidade Estadual de Campinas, Campinas, 1996 (dissertação de mestrado).
[18] K. Bruce, B.K. Gullett, L.O. Beach, Comparative SO_2 reactivity of CaO derived from $CaCO_3$ and $Ca(OH)_2$, AlChE J. 35 (1989) 37–41.
[19] A. Al-Shawabkeh, H. Matsuda, M. Hasatani, Comparative reactivity of $Ca(OH)_2$—derived oxides for SO_2 capture, J. Chem. Eng. Jpn. 7 (1994) 650–656.
[20] D. Geldart, Gas Fluidization Technology, Wiley, Chichester, 1986.
[21] K. Kato, H. Sakamoto, H. Sakurai, T. Takarada, N. Nakagawa, Effective dry desulfurization by a powder-particle fluidized-bed, J. Chem. Eng. Jpn. 27 (1994) 276–278.
[22] T. Tashimo, H. Machida, Y. Matsumoto, N. Nakagawa, K. Kato, Desulfurization characteristics in a high-temperature powder-particle fluidized bed desulfurizer, Kagaku Kogaku Ronbunshu 24 (1998) 324–328.
[23] D. Kunii, O. Levenspiel, Fluidization Engineering, second ed., Butterworth-Heinemann, Boston, 1991.
[24] K. Kato, T. Takarada, N. Matsuo, T. Suto, Residence-time distribution of fine particles in a powder-particle fluidized bed, Int. Chem. Eng. 34 (1994) 605–610.
[25] R. Pisani Jr., D. Moraes Jr., Removal of SO_2 with particles of dolomite limestone powder in a binary fluidized bed reactor with bubbling fluidization, Braz. J. Chem. Eng. 20 (2003) 95–103.
[26] P. Cai, S.P. Chen, Y. Jin, Z.Q. Yu, W. Wang, Effect of operation temperature and pressure on the transition from bubbling to turbulent fluidization, AlChE Symp. Ser. 85 (1989) 37–43.
[27] D. Bai, Y. Masuda, N. Nakagawa, K. Kato, Hydrodynamic behavior of a binary solids fluidized bed, J. Chem. Eng. Jpn. 29 (1996) 211–216.
[28] R.G. Casqueira, Tratamento do poluente gasoso dióxido de enxofre com a cal hidratada em um leito fluidizado binário, Universidade Federal de São Carlos, São Carlos, 1999 (dissertação de mestrado).
[29] R.H. Borgwardt, K.R. Bruce, Effect of specific surface area on the reactivity of CaO with SO_2, AlChE J. 32 (1986) 239–246.
[30] C. Hsia, G.R.S. Pierre, L.S. Fan, Isotope study on $CaSO_4$ formed during sorbent-flue-gas reaction, AlChE J. 41 (1995) 2337–2340.